TẠP CHÍ KHOA HỌC
TRƯỜNG ĐẠI HỌC QUY NHƠN

Hiểu biết sâu sắc hơn về độ bền và đặc trưng của các liên kết hydrogen O/C_{sp2}-H···Z trong các hệ phức tương tác giữa dẫn xuất của chalcogenoaldehyde acid và formamide

Lê Thị Tú Quyên[1], Bùi Đức Ái[1], Trần Mạnh Trung[1], Phạm Ngọc Thạch[1,2], Nguyễn Tiến Trung[1,2,*]

[1]Phòng Thí nghiệm Hóa học tính toán và Mô phỏng, Trường Đại học Quy Nhơn, Việt Nam
[2]Khoa Khoa học Tự nhiên, Trường Đại học Quy Nhơn, Việt Nam

Ngày nhận bài: 11/03/2025; Ngày sửa bài: 14/04/2025;
Ngày nhận đăng: 16/04/2025; Ngày xuất bản: 28/06/2025

TÓM TẮT

Các cấu trúc bền của các phức tương tác giữa RCZOH và NH_2CHZ, với R = H, F, CH_3 và Z = O, S, Se và Te đã được tìm thấy trong nghiên cứu này. Độ bền của các liên kết hydrogen O/C_{sp2}-H···Z có xu hướng giảm dần khi Z lần lượt là O, S, Se, và Te. Sự chuyển dời đỏ tần số dao động hóa trị của liên kết O-H trong các liên kết hydrogen O-H···O lớn hơn so với các liên kết hydrogen O-H···S/Se/Te, trong đó sự chuyển dời đỏ O-H rất lớn đạt đến 958,0 cm^{-1} được phát hiện ở các liên kết hydrogen O-H···O. Mức độ chuyển dời đỏ O-H càng tăng khi nhóm thế Z trong RCZOH đi từ O đến Te và R chuyển từ nhóm đẩy electron CH_3 sang nhóm thế hút electron F. Đáng chú ý, sự chuyển dời xanh đáng kể của C_{sp2}-H lên đến 104,9 cm^{-1} trong liên kết hydrogen không cổ điển C_{sp2}-H···O đã được quan sát thấy. Tần số dao động hóa trị của C_{sp2}-H trong các liên kết hydrogen C_{sp2}-H···S/Se/Te có xu hướng đi từ chuyển dời xanh sang chuyển dời đỏ khi nhóm thế Z trong NH_2CHZ dần được thay thế từ O đến Te. Đặc biệt, ái lực proton tại phần tử nhận proton Z và độ phân cực của phần tử cho proton O/C_{sp2}-H càng tăng thì mức độ chuyển dời đỏ của O/C_{sp2}-H càng rõ rệt và ngược lại.

Từ khóa: *Liên kết hydrogen cổ điển, liên kết hydrogen không cổ điển, chuyển dời đỏ, chuyển dời xanh, NBO.*

**Tác giả liên hệ chính.*
Email: nguyentientrung@qnu.edu.vn

https://doi.org/10.52111/qnjs.2025.19304

QUY NHON UNIVERSITY
JOURNAL OF SCIENCE

An insight into stability and characteristics of O/C_{sp2}-H···Z hydrogen bonds in the binary systems of chalcogenocarboxylic acid and formamide derivatives

Le Thi Tu Quyen[1], Bui Duc Ai[1], Tran Manh Trung[1], Pham Ngoc Thach[1,2], Nguyen Tien Trung[1,2,*]

[1]Laborabory of Computational Chemistry and Modelling, Quy Nhon University, Vietnam
[2]Faculty of Natural Sciences, Quy Nhon University, Vietnam

Received: 11/03/2025; Revised: 14/04/2025;
Accepted: 16/04/2025; Published: 28/06/2025

ABSTRACT

Forty-eigth stable structures of complexes were identified for interaction of RCZOH and NH_2CHZ, with R= H, F, CH_3 and Z= O, S, Se, Te. Strength of O/C_{sp2}-H···Z hydrogen bonds decreases in the order of the Z acceptors: O > S > Se > Te. The O-H stretching frequency's red shifts of the O-H···O hydrogen bonds are larger than those of the O-H···S/Se/Te ones, in which the significant O-H red shift of 958.0 cm^{-1} is detected in the O-H···O ones. There is an increase in the O-H red shift as Z in the RCZOH goes from O to Te, and R changes from the electron-donating CH_3 group to the electron-withdrawing F substituent. Remarkably, a substantial blue shift of the C_{sp2}-H up to 104.9 cm^{-1} in the nonconventional C_{sp2}-H···O hydrogen bond is found, and an obvious trend from blue shift to red shift of C_{sp2}-H stretching frequencies in the C_{sp2}-H···S/Se/Te hydrogen bonds is also detected as Z in the NH_2CHZ varying from the O to Te substituent. It is noteworthy that the proton affinity at the Z proton acceptors and the polarity of the O/C_{sp2}-H proton donors increase along with the enhancement of the O/C_{sp2}-H red shift, and *vice versa.*

Keywords: *Conventional hydrogen bonds, nonconventional hydrogen bonds, red shift, blue shift, NBO.*

1. INTRODUCTION

Hydrogen bond is one of the noncovalent interactions, playing essential roles in chemistry, physics, and biological systems such as DNA, RNA, or protein.[1,2] The importance of hydrogen bonds especially appears in biochemical reactions, supermolecule synthesis, and crystal design.[2–4] Therefore, a thorough understanding of hydrogen bonds can expand their application in various fields of life.

Up to now, the A-H···B hydrogen bonds have had two main types, including conventional, and nonconventional hydrogen bonds. Therein, the A and B atoms in the conventional hydrogen bonds often possess high electronegativity or electron-rich regions. This type of hydrogen bonds is usually characterised by a stretching frequency red shift of the proton donor, which is displayed by an increase in the A-H bond length and a decrease of its stretching frequency.[4,5] By contrast, either or both A and B in the nonconventional hydrogen bonds have low electronegativity or lower electron density regions.[5,6] Notably, the nonconventional hydrogen bonds not only show the attributes of

**Corresponding author.*
Email: nguyentientrung@qnu.edu.vn

https://doi.org/10.52111/qnjs.2025.19304

the red shift but also present the blue shift of stretching frequency, named the blue-shifting hydrogen bonds. The blue-shifting hydrogen bond is associated with a contraction of the proton donor bond length and an enhancement of its stretching frequency. [7,8]

The nature of hydrogen bonds, especially the blue-shifting ones, has been investigated both by experimental and theoretical methods. [6,7,9,10] Therein, some studies showed that attaching either electron-donating or electron-withdrawing groups to the C-H proton donors may change the electron density of the C-H bond, [11–13] affecting the strength and characteristics of hydrogen bonds. Noted that the blue shifts of the C_{sp2}-H bonds are very large and even surpass those of the C_{sp3}-H bonds.[11,14] Indeed, the increase in the C_{sp2}-H bond's stretching frequency of the nonconventional C_{sp2}-H···O/S hydrogen bonds in the range of 81 – 96 cm^{-1} was reported for the complexes of HCOOH with XCHZ (X= H, F, Cl, Br, CH_3, NH_2; Z= O, S).[11] Besides, a huge blue shift of the C_{sp2}-H bond up to 104.5 cm^{-1} was obtained in the FCOOH···CH_3CHO complex.[15] The characteristics of nonconventional C_{sp2}-H···Se/Te, and O-H···Se/Te hydrogen bonds were also investigated in some recent studies. For instance, the nonconventional C_{sp2}-H···Se/Te and O-H···Se/Te hydrogen bonds were found by Cuc *et al* in XCHZ···nH_2O (X= H, F, Cl, Br, CH_3; Z= O, S, Se, Te; n = 1-3) and XCHO···nH_2Z (X= H, F, Cl, Br, CH_3; Z= O, S, Se, Te; n = 1-2) complexes.[16,17] It is interesting that these nonconventional hydrogen bonds are characterized by the red shifts. Likewise, Quyen *et al* had observed the red shifts of the C_{sp2}-H···Se/Te hydrogen bonds in the dimer of chalcogenoaldehyde derivatives and complexes of XCHZ···RCZOH (X= H, F; R= H, F, Cl, Br, CH_3, NH_2; Z= O, S, Se, Te) recently.[18,19] These reports pave the way for more studies on the stability and nature of nonconventional hydrogen bonds with heavy chalcogen atoms playing as proton acceptors. Specially, Mishra *et al* discovered the existence and red shifts of nonconventional N-H···Se and O-H···Se hydrogen bonds both experimentally and computationally in the interactions of indole···dimethyl selenide, and phenol···dimethyl selenide.[20] Therefore, it is necessary to investigate the hydrogen bonds containing chalcogen atoms in various complexes to provide fundamental knowledge to exploit their applications in other fields.

Remarkably, Trung *et al* suggested that the strength and characteristics of nonconventional C-H···Z hydrogen bonds involve the inherent properties of the C-H proton donor, and the Z proton acceptor. In particular, the C-H stretching frequency's shift of these nonconventional hydrogen bonds can be predicted thanks to polarity of the proton donors, and proton affinity of the proton acceptors.[21–24] This model has provided a quick sign to detect characteristics of the hydrogen bonds. These observations lead to an idea of studying the interaction and characteristics of conventional and nonconventional hydrogen bonds in complexes between NH_2CHZ and RCZOH with R= H, F, CH_3; Z= O, S, Se, Te by using quantum computational approach in order to have a more obvious understanding of origin of nonconventional hydrogen bonds. In addition, the system is chosen for investigation because as mentioned above some chalcogenoaldehydes substituted by electron-donating group and carboxylic acids replaced by electron-withdrawing one cause a blue shift of C-H bond involving in the hydrogen bond. Furthermore, studying different R and Z substituents can help to clarify their impact on the inherent properties of proton donors and proton acceptors which could be considered as one of the reasons for the various characteristics of nonconventional hydrogen bonds. The strength and nature of nonconventional O-H···Se/Te, and C_{sp2}-H···Z (Z= O, S, Se, Te) hydrogen bonds are also highlighted in the present work.

https://doi.org/10.52111/qnjs.2025.19304

2. COMPUTATIONAL METHODS

The geometrical structures of the monomers and investigated complexes were optimized using the second-order perturbation theoretical method (MP2)[25] with the pseudopotential basis set aug-cc-pVDZ-PP for Te,[26] and full-electron Pople basis set 6-311++G(3df,2pd) for the other atoms through the Gaussian 16 program.[27] The infrared spectra for both complexes and monomers were then calculated at the same level of theory. Interaction energies of the complexes were computed as the following expression:

$$\Delta E^{*} = (E + ZPE)_{complex} - \sum(E + ZPE)_{monomer} + BSSE$$

In which the single-point energy of the complex and monomer (E), and the basis set superposition error (BSSE) correction were calculated using couple cluster CCSD(T) method. The zero-point vibrational energies (ZPE) were obtained at the optimized geometries of the molecule. The deprotonation enthalpy (DPE) and the proton affinity (PA) were respectively computed for the proton donors C_{sp2}/O-H and the proton acceptors Z in the monomers using CCSD(T) method in combination with the 6-311++G(3df,2pd) basis set, except the aug-cc-pVDZ-PP applied for the Te atom. These parameters will be used to evaluate polarity of the proton donors C_{sp2}/O-H and proton affinity of the proton acceptors Z in the isolated monomers.

Moreover, the formation and strength of hydrogen bonds in complexes were determined by the AIMall program[28,29] using MP2 method with the aug-cc-pVDZ-PP basis set for Te atom, and the 6-311++G(3df,2pd) for the remaining atoms. This analysis showed the bond critical points (BCPs) which could explicitly prove the existence of hydrogen bonds. Some typical parameters at BCPs such as electron density ρ(r), Laplacian electron density $\nabla^2\rho(r)$, and potential energy density V(r) were collected to evaluate for the strength of hydrogen bonds on the basis of the emprical formula: $E_{HB} = 0.5V(r)$,[30] with E_{HB} being the energy of individual hydrogen bonds. Natural bond orbital (NBO) analysis [31] was also applied utilizing the same level of theory as for the AIM analysis. The NBO analysis provides data on intermolecular electron density transfer between two monomers, changes in electron density of a specific orbital and atomic charges.

3. RESULTS AND DISCUSSION

3.1. Geometrical structures and AIM analysis

Interaction of RCZOH with NH_2CHZ (with R= H, F, CH_3; Z= O, S, Se, Te) induces 48 stable complexes with the similar structures shown in Figure 1a. These structures are symbolized as **RZ2-Z7**, with R being H, F, and CH_3; Z2 and Z7 being O, S, Se, and Te atoms in the RCZOH and NH_2CHZ monomers, respectively. All the complexes are stabilized by two intermolecular interactions O-H···Z7 and C_{sp2}-H···Z2. The topological features obtained from the AIM analysis point out the presence of bond critical points (BCPs) between H and Z atoms, and ring critical point (RCP) in complexes as displayed in Figure 1b. The intermolecular distances of H···O, H···S, H···Se, and H···Te contacts are smaller than their sum of Van der Waals radii, affirming the existence of the O-H···Z7 and C_{sp2}-H···Z2 interactions and ring-shaped structures following the complexation.

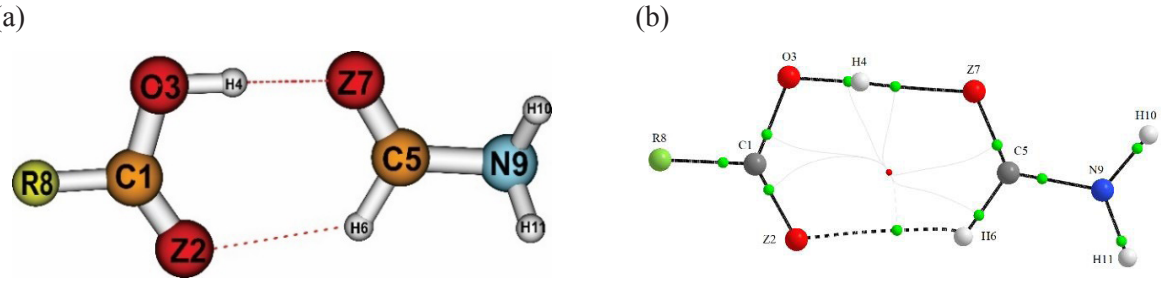

Figure 1. (a) The stable geometrical structures and (b) their topological analysis of RCZOH···NH_2CHZ complexes, with R= H, F, CH_3; Z= O, S, Se, Te.

The data from AIM analysis in Tables S1a, and S1b of Supporting Information (SI) showed the values of electron density ($\rho(r)$) and Laplacian of electron density ($\nabla^2\rho(r)$) at the BCPs of the O-H···Z7 interactions being 0.022 – 0.068 au and 0.026 – 0.109 au, respectively. The $\rho(r)$ and $\nabla^2\rho(r)$ values for the C_{sp2}-H···Z2 interactions are 0.009-0.017 au , and 0.021 – 0.063 au, respectively, which are smaller than those of the O-H···Z7 contacts. In general, these parameters belong to the range of the hydrogen bond formation.[32] Accordingly, the O-H···Z7, and C_{sp2}-H···Z2 intermolecular interactions in the investigated complexes are tentatively assumed as hydrogen bonds, and the formers are much more stable than the latters. This is evidenced by the much more negative E_{HB} values of the O-H···Z7 hydrogen bonds (-16.0 to -101.3 kJ.mol^{-1}) compared to the C_{sp2}-H···Z2 ones (-5.3 to -16.4 kJ.mol^{-1}) (*cf.* Tables S1a, and 1b). The negative values of the local electron energy density (H(r)) at BCPs of the O-H···Z7 reflect their partially covalent character (*cf.* Table S1b). The larger strength of O-H···Z relative to C_{sp2}-H···Z was also suggested in the RCZOH···CH_3CHZ (R= H, F, CH_3; Z= O, S) [15] and RCZOH···FCHZ (R= H, F, Cl, Br, CH_3, NH_2; Z= O, S, Se, Te) complexes.[18] The energies of the individual C_{sp2}-H···O/S and O-H···O/S hydrogen bonds calculated at MP2/6-311++G(3df,2pd) in the RCZOH···CH_3CHZ complexes were indeed in the ranges of -6.4 ÷ -13.5 kJ.mol^{-1}, and -23.9 ÷ -71.8 kJ.mol^{-1}, respectively.[15] This indicates that replacement of the CH_3 group in the CH_3CHZ with a group that exerts a stronger electron-donating conjugation effect, such as NH_2, induces an increase in the strength of the O/C_{sp2}-H···Z hydrogen bonds.

For the nonconventional C_{sp2}-H···Z2 hydrogen bonds, their strength decrease in the order of Z2 substituents O >> S > Se > Te upon fixing R and Z7 groups. This order agrees well with the less negative of E_{HB} when Z2 goes from O to S to Se and then to Te (*cf.* Table S1a). Indeed, the E_{HB} values of C_{sp2}-H···S2/Se2/Te2 range from -5.3 to -9.7 kJ.mol^{-1}, which are less negative than those of C_{sp2}-H···O2 (from -11.2 to -16.4 kJ.mol^{-1}). A similar observation was also obtained in the studies of Quyen *et al*,[18] and An *et al*.[15] This result emphasizes the importance of the oxygen compared to sulfur, selenium, and tellurium as Z2 in the stability of the nonconventional C_{sp2}-H···Z2 hydrogen bonds. In contrast, for the same R and Z2, the strength of C_{sp2}-H···Z2 tends to increase along with the shortening in intermolecular distance H···Z2 when Z7 turns from O via S via Se and then Te (*cf.* Figure S1a). The similar observation was found in the complexes of $CYHNH_2$ with XH (Y= O, S, Se, Te; X= F, HO, NH_2).[12] It is noteworthy that the DPE values of the C_{sp2}-H bonds in the monomers decrease in the order NH_2CHO > NH_2CHS > NH_2CHSe > NH_2CHTe (*cf.* Table 1), implying the polarity of C_{sp2}-H bonds in the NH_2CHZ increase in the sequence of Z7 substituents O < S < Se < Te. Figure S1a also reflects the weakening of C_{sp2}-H···Z2 hydrogen bonds in the order **CH_3Z2-Z7** > **HZ2-Z7** > **FZ2-Z7** with Z2 and Z7 being O, S and Se, whereas the strength of C_{sp2}-H···Te2 in the **HTe2-O7**, **FTe2-O7**, and **CH_3Te2-O7** are almost similar. This comparison suggests that for the same Z2 and Z7, the stronger C_{sp2}-H···Z2 hydrogen bonds are obtained for R being the electron-donating CH_3 substituent than the electron-withdrawing F one.

Table 1. Deprotonation enthalpy (DPE) of O/C_{sp2}-H bond, and proton affinity at proton acceptors Z in NH_2CHZ and RCZOH monomers with R= H, F, CH_3; Z= O, S, Se, Te.

Monomer	PA(Z) (kJ.mol^{-1})	DPE(O/C–H) (kJ.mol^{-1})	Monomer	PA(Z) (kJ.mol^{-1})	DPE(O/C–H) (kJ.mol^{-1})
CH_3COOH	823.7	1495.1	**FCOOH**	736.9	1406.9
CH_3CSOH	840.6	1433.0	**FCSOH**	780.8	1351.6
CH_3CSeOH	840.0	1406.0	**FCSeOH**	785.5	1327.1
CH_3CTeOH	864.9	1382.0	**FCTeOH**	825.6	1302.4
HCOOH	780.1	1480.4	**NH_2CHO**	873.2	1668.4
HCSOH	805.8	1421.4	**NH_2CHS**	888.3	1625.3
HCSeOH	806.2	1396.5	**NH_2CHSe**	882.8	1605.4
HCTeOH	839.0	1374.2	**NH_2CHTe**	909.6	1587.8

Regarding the O-H···Z7 hydrogen bonds, for the same R and Z2, their strength decreases in the order of the Z7 groups: O > S > Se > Te. This result agrees with the observations of Biswal *et al*, and Das *et al* in previous reports.[33,34] The atomic charges at the Z7 atoms in the investigated complexes become less negative when Z7 goes from O to Te (*cf.* Table S2), leading to a descending in the electrostatic attraction of H4···Z7 in the sequence H4···O7 > H4···S7 > H4···Se7 > H4···Te7. This tendency is one of the reasons for the superior strength of O-H···O7 relative to O-H···S7/Se7/Te7. For the same R and Z7, the O-H···Z7 hydrogen bonds experience an enhancement in their strength when Z2 varies from O to S, to Se, and then to Te. This observation is consistent with the increase of O-H polarity in the order RCOOH < RCSOH < RCSeOH < RCTeOH (*cf.* Table 1). Thus, the polarity of O-H bonds and the strength of O-H···Z7 hydrogen bonds are affected by the Z7 atom in the RCZOH monomers, in which, Te7 is more influential than O7, S7 or Se7. Notably, the strength of O-H···Z7 goes down when R changes from F to H and then CH_3, being opposite to the tendency observed for C_{sp2}-H···Z2 hydrogen bonds (*cf.* Figures S1a, and S1b). This is reasonable because F surpasses CH_3 group in raising the polarity of O-H bonds (*cf.* Table 1) and the electrostatic attraction between H4 and Z7. Consequently, the electron-withdrawing substituent (F) induces stronger O-H···Z7 hydrogen bonds than the electron-donating one (CH_3). This effect was also reflected in the complexes of XCHZ···RCZOH (with X= H, F; R= H, F, Cl, Br, CH_3, NH_2; Z= O, Se, Se, Te).[18]

3.2. Interaction energy

The interaction energies corrected by both ZPE and BSSE (denoted by ΔE^*) of **RZ2-Z7** complexes are calculated at the CCSD(T)/6-311++G(3df,2pd)//MP26-311++G(3df,2pd) level of theory (except the aug-cc-pVDZ-PP basis set used for Te atom) to evaluate the stability of investigated complexes. The data in Table 2 shows the negative interaction energies of complexes ranging from -30.9 to -73.8 kJ.mol^{-1}, indicating their certain stability on their potential energy surfaces.

For the same R and Z2, the individual interaction energies of **RZ2-O7**, **RZ2-S7**, **RZ2-Se7**, and **RZ2-Te7** are in the ranges -44.5 ÷ -73.8 kJ.mol^{-1}, -34.8 ÷ -55.5 kJ.mol^{-1}, -32.9 ÷ -55.8 kJ.mol^{-1}, and -31.3 ÷ -47.0 kJ.mol^{-1}, respectively. These values indicates that the stability of **RZ2-Z7** complexes decreases in the order of Z7 substituents: O > S > Se > Te, which is consistent with the lowering strength of O-H···Z7 in the sequence: O-H···O7 >> O-H···S7 > O-H···Se7 > O-H···Te7 as resulted from the AIM analysis. This observation emphasizes a predominant influence of the oxygen compared to sulfur, selenium, or tellurium as Z7 on the stability of **RZ2-Z7**. Besides, the superior role of the O-H···Z7 hydrogen bonds relative to C_{sp2}-H···Z2 in stabilizing complexes is noticed.

https://doi.org/10.52111/qnjs.2025.19304

Table 2. Interaction energies corrected by both ZPE and BSSE (ΔE*, kJ.mol^{-1}) of complexes between NH_2CHZ and RCZOH (R = H, F, CH_3; Z = O, S, Se, Te) at CCSD(T)/6-311++G(3df,2pd)//MP2/6-311++G(3df,2pd)) level of theory (except the aug-cc-pVDZ-PP basis set used for Te atom).

Complex	ΔE*	Complex	ΔE*	Complex	ΔE*	Complex	ΔE*
CH_3O2–O7	-44.5	**CH_3O2–S7**	-36.7	**CH_3O2–Se7**	-35.3	**CH_3O2–Te7**	-43.5
CH_3S2–O7	-44.7	**CH_3S2–S7**	-34.8	**CH_3S2–Se7**	-32.9	**CH_3S2–Te7**	-40.1
CH_3Se2–O7	-46.3	**CH_3Se2–S7**	-35.7	**CH_3Se2–Se7**	-34.2	**CH_3Se2–Te7**	-42.2
CH_3Te2–O7	-55.3	**CH_3Te2–S7**	-44.2	**CH_3Te2–Se7**	-45.0	**CH_3Te2–Te7**	-31.3
HO2–O7	-46.3	**HO2–S7**	-37.4	**HO2–Se7**	-35.8	**HO2–Te7**	-40.2
HS2–O7	-47.6	**HS2–S7**	-35.1	**HS2–Se7**	-33.1	**HS2–Te7**	-36.6
HSe2–O7	-47.2	**HSe2–S7**	-36.2	**HSe2–Se7**	-34.5	**HSe2–Te7**	-38.9
HTe2–O7	-55.2	**HTe2–S7**	-44.1	**HTe2–Se7**	-44.8	**HTe2–Te7**	-30.9
FO2–O7	-58.9	**FO2–S7**	-46.1	**FO2–Se7**	-44.6	**FO2–Te7**	-47.0
FS2–O7	-60.0	**FS2–S7**	-44.2	**FS2–Se7**	-42.3	**FS2–Te7**	-43.6
FSe2–O7	-63.2	**FSe2–S7**	-46.0	**FSe2–Se7**	-44.3	**FSe2–Te7**	-46.3
FTe2–O7	-73.8	**FTe2–S7**	-55.5	**FTe2–Se7**	-55.8	**FTe2–Te7**	-40.7

For the same R and Z7, the more negative interaction energies of **RZ2-O7**, **RZ2-S7**, and **RZ2-Se7** are observed for the Z2 being the Te atom rather than the O, S, and Se (*cf.* Table 2), in line with the decreasing strength of O-H···Z7 hydrogen bonds when Z2 goes from Te to O. However, an opposite trend is obtained for **RZ2-Te7** complexes, in which, **RO2-Te7** is more stable than **RSe2-Te7**, **RS2-Te7**, and **RTe2-Te7** (*cf.* Table 2).

Fixing Z2 and Z7, the interaction energies of **FZ2-Z7** are more negative than those of **HZ2-Z7** and **CH_3Z2-Z7**. Indeed, the ΔE* values range from -40.7 to -73.8 kJ.mol^{-1} for **FZ2-Z7**, from -30.9 to -55.2 kJ.mol^{-1} for **HZ2-Z7**, and from -31.3 to -55.3 kJ.mol^{-1} for **CH_3Z2-Z7** (*cf.* Table 2). This implies that replacing R in the RCZOH with F can strengthen the stability of **RZ2-Z7** more than CH_3 which is also consistent with the larger strength of O-H···Z7 hydrogen bonds in **FZ2-Z7** compared to that of **CH_3Z2-Z7**. Therefore, this observation affirms the crucial role of O-H···Z7 hydorgen bonds in the stability of the investigated complexes.

3.3. NBO analysis

To evaluate the electron density transfer between monomers upon the complexation, the NBO analysis is performed and the selected data are gathered in Tables 3a, and 3b. The total electron density transfer (EDT) of NH_2CHZ monomers ranging from 0.036 to 0.091 indicates electron density transferring mainly from NH_2CHZ to RCZOH. This is proven by the intermolecular hyperconjugative energy (E_{inter}) of electron transter from nonbonding orbital n(Z7) to σ*(O-H) antibonding orbital (*ca.* 85.3-252.0 kJ.mol^{-1}) surpasses that from n(Z2) to σ*(C_{sp2}-H) (*ca.* 6.8-21.2 kJ.mol^{-1}), confirming the larger strength of O-H···Z7 compared to that of C_{sp2}-H···Z2 hydrogen bonds.

For the same R and Z7, the E_{inter} values of the electron density transfer from n(Z2) to σ*(C_{sp2}-H) increase in the order of the Z2 substituents: O < S < Se < Te (*cf.* Tables 3a, and 3b), which is in a consistent with the enhancement of proton affinity at Z2 in the order RCOOH < RCSOH < RCSeOH < RCTeOH (*cf.* Table 1). This order is opposite to the strength tendency of C_{sp2}-H···Z2 hydrogen bonds. Therefore, the higher strength of C_{sp2}-H···O2 compared to C_{sp2}-H···S2/Se2/Te2 hydrogen bonds is primarily determined by the electrostatic attraction rather than the intermolecular electron density transfer. The outstanding contribution of electrostatic attraction compared to the intermolecular electron density transfer on the strength of C_{sp2}-H···Z hydrogen bonds was also pointed out in the XCHZ···RCZOH complexes (with X= H, F; R= H, F, Cl, Br, CH_3, NH_2; Z= O, S, Se, Te) by Quyen *et al*.[18] When fixing R and Z2, the E_{inter} values of the nonconventional C_{sp2}-H···Z2 hydrogen bonds go up as Z7 varies from O to Te, which is in line with the strength of C_{sp2}-H···Z2 hydrogen bonds.

https://doi.org/10.52111/qnjs.2025.19304

Table 3a. Data from NBO analysis of **RZ2-Z7** complexes with R= H, F, CH_3; Z= O, S.

Complex	Hydrogen bond	EDT [(a)] (Electron)	E_{inter} (kJ.mol^{-1})	ΔE_{intra} [(b)] (kJ.mol^{-1})	$\Delta\sigma^*(C_{sp2}/O\text{-}H)$ (Electron)	$\Delta\%s(C_{sp2})$
CH_3O2-O7	C5-H6···O2	0.036	8.3	-34.9	-0.0106	1.4
	O3-H4···O7		126.4	1.2	0.0388	4.8
CH_3S2-O7	C5-H6···S2	0.037	12.3	-33.0	-0.0062	1.3
	O3-H4···O7		145.9	2.1	0.0418	5.2
CH_3Se2-O7	C5-H6···Se2	0.039	13.5	-34.4	-0.0059	1.3
	O3-H4···O7		157.0	0.3	0.0441	5.3
CH_3Te2-O7	C5-H6···Te2	0.040	15.7	-34.9	-0.0047	1.3
	O3-H4···O7		162.9	0.3	0.0447	5.5
HO2-O7	C5-H6···O2	0.039	8.3	-35.5	-0.0106	1.4
	O3-H4···O7		140.3	0.0	0.0416	4.9
HS2-O7	C5-H6···S2	0.039	12.4	-33.6	-0.0060	1.3
	O3-H4···O7		156.0	-1.3	0.0434	5.4
HSe2-O7	C5-H6···Se2	0.041	13.7	-34.9	-0.0056	1.3
	O3-H4···O7		166.4	-1.5	0.0455	5.6
HTe2-O7	C5-H6···Te2	0.040	15.9	-34.9	-0.0042	1.3
	O3-H4···O7		170.7	-1.3	0.0450	5.7
FO2-O7	C5-H6···O2	0.052	6.8	-39.4	-0.0126	1.3
	O3-H4···O7		184.9	6.5	0.0540	5.0
FS2-O7	C5-H6···S2	0.055	11.5	-39.3	-0.0090	1.3
	O3-H4···O7		211.6	-1.6	0.0602	5.3
FSe2-O7	C5-H6···Se2	0.059	13.4	-41.6	-0.0086	1.4
	O3-H4···O7		231.5	0.6	0.0649	5.5
FTe2-O7	C5-H6···Te2	0.061	16.9	-43.1	-0.0072	1.5
	O3-H4···O7		252.0	-1.5	0.0686	5.6
CH_3O2-S7	C5-H6···O2	0.049	14.8	-19.4	-0.0050	1.8
	O3-H4···S7		112.9	4.4	0.0534	4.7
CH_3S2-S7	C5-H6···S2	0.051	18.3	-16.1	0.0010	1.7
	O3-H4···S7		132.9	12.9	0.0604	5.1
CH_3Se2-S7	C5-H6···Se2	0.055	19.3	-16.3	0.0016	1.7
	O3-H4···S7		143.3	8.6	0.0642	5.3
CH_3Te2-S7	C5-H6···Te2	0.057	21.2	-15.6	0.0030	1.7
	O3-H4···S7		148.5	9.3	0.0657	5.5
HO2-S7	C5-H6···O2	0.055	14.5	-19.2	-0.0049	1.7
	O3-H4···S7		125.2	3.4	0.0583	4.9
HS2-S7	C5-H6···S2	0.055	18.2	-16.1	0.0013	1.6
	O3-H4···S7		143.5	10.0	0.0641	5.4
HSe2-S7	C5-H6···Se2	0.059	19.3	-16.3	0.0020	1.7
	O3-H4···S7		153.6	8.1	0.0678	5.6
HTe2-S7	C5-H6···Te2	0.059	21.1	-15.5	0.0035	1.7
	O3-H4···S7		156.2	8.1	0.0681	5.8
FO2-S7	C5-H6···O2	0.075	11.7	-20.2	-0.0070	1.7
	O3-H4···S7		165.1	-0.2	0.0754	5.4
FS2-S7	C5-H6···S2	0.078	15.9	-17.8	-0.0019	1.6
	O3-H4···S7		186.8	6.1	0.0840	5.8
FSe2-S7	C5-H6···Se2	0.083	17.5	-18.3	-0.0011	1.7
	O3-H4···S7		200.7	9.0	0.0898	6.0
FTe2-S7	C5-H6···Te2	0.086	20.7	-18.1	0.0006	1.8
	O3-H4···S7		210.3	7.2	0.0936	6.1

(a) The total electron density transfer from NH_2CHZ to RCZOH

(b) The total intramolecular electron density transfer to the $\sigma^*(C_{sp2}/O\text{-}H)$ orbitals

https://doi.org/10.52111/qnjs.2025.19304

Table 3b. Data from NBO analysis of **RZ2-R7** complexes, with R= H, F, CH_3; Z= Se, Te.

Complex	Hydrogen bond	EDT [(a)] (Electron)	E_{inter} (kJ.mol^{-1})	ΔE_{intra} [(b)] (kJ.mol^{-1})	$\Delta\sigma^*(C_{sp2}/O\text{-}H)$ (Electron)	$\Delta\%s(C_{sp2})$
CH_3O2-Se7	C5-H6···O2	0.044	15.1	-16.3	-0.0031	1.8
	O3-H4···Se7		98.1	4.9	0.0494	4.4
CH_3S2-Se7	C5-H6···S2	0.048	17.7	-12.8	0.0026	1.7
	O3-H4···Se7		119.2	11.5	0.0574	5.0
CH_3Se2-Se7	C5-H6···Se2	0.052	18.5	-12.7	0.0032	1.7
	O3-H4···Se7		129.3	12.7	0.0617	5.2
CH_3Te2-Se7	C5-H6···Te2	0.060	20.5	-10.8	0.0051	1.7
	O3-H4···Se7		149.1	12.9	0.0692	5.6
HO2-Se7	C5-H6···O2	0.051	14.7	-16.1	-0.0031	1.7
	O3-H4···Se7		110.0	6.3	0.0546	4.7
HS2-Se7	C5-H6···S2	0.052	17.5	-12.8	0.0028	1.7
	O3-H4···Se7		129.4	11.5	0.0616	5.3
HSe2-Se7	C5-H6···Se2	0.057	18.3	-12.8	0.0035	1.7
	O3-H4···Se7		139.0	11.7	0.0655	5.5
HTe2-Se7	C5-H6···Te2	0.063	20.4	-10.6	0.0055	1.7
	O3-H4···Se7		155.9	9.5	0.0716	5.9
FO2-Se7	C5-H6···O2	0.072	11.6	-16.7	-0.0050	1.7
	O3-H4···Se7		146.4	0.3	0.0717	5.3
FS2-Se7	C5-H6···S2	0.076	14.9	-13.8	-0.0001	1.6
	O3-H4···Se7		168.6	6.8	0.0810	5.7
FSe2-Se7	C5-H6···Se2	0.081	16.4	-14.1	0.0007	1.7
	O3-H4···Se7		181.9	9.9	0.0872	6.0
FTe2-Se7	C5-H6···Te2	0.090	19.6	-12.6	0.0029	2.1
	O3-H4···Se7		207.4	8.4	0.0976	6.3
CH_3O2-Te7	C5-H6···O2	0.040	14.6	-12.0	-0.0018	1.8
	O3-H4···Te7		85.3	5.9	0.0459	4.1
CH_3S2-Te7	C5-H6···S2	0.047	16.2	-8.8	0.0035	1.7
	O3-H4···Te7		110.3	16.4	0.0572	4.7
CH_3Se2-Te7	C5-H6···Se2	0.053	18.4	-8.7	0.0048	1.8
	O3-H4···Te7		123.1	15.8	0.0637	5.1
CH_3Te2-Te7	C5-H6···Te2	0.058	18.1	-7.5	0.0054	1.8
	O3-H4···Te7		130.1	15.9	0.0667	5.3
HO2-Te7	C5-H6···O2	0.047	14.0	-11.7	-0.0018	1.7
	O3-H4···Te7		96.1	7.8	0.0516	4.4
HS2-Te7	C5-H6···S2	0.052	15.7	-13.2	0.0036	1.7
	O3-H4···Te7		118.6	11.2	0.0614	5.1
HSe2-Te7	C5-H6···Se2	0.057	18.0	-8.7	0.0049	1.8
	O3-H4···Te7		131.7	15.2	0.0680	5.4
HTe2-Te7	C5-H6···Te2	0.060	17.7	-7.5	0.0056	1.7
	O3-H4···Te7		136.0	14.9	0.0695	5.6
FO2-Te7	C5-H6···O2	0.071	10.7	-11.7	-0.0036	1.6
	O3-H4···Te7		132.1	5.4	0.0704	5.1
FS2-Te7	C5-H6···S2	0.079	13.1	-9.0	0.0010	1.6
	O3-H4···Te7		158.3	10.9	0.0832	5.7
FSe2-Te7	C5-H6···Se2	0.086	15.7	-9.2	0.0023	1.7
	O3-H4···Te7		173.8	16.6	0.0917	6.0
FTe2-Te7	C5-H6···Te2	0.091	16.6	-8.3	0.0033	1.8
	O3-H4···Te7		183.6	14.6	0.0969	6.3

(a) The total electron density transfer from NH_2CHZ to RCZOH

(b) The total intramolecular electron density transfer to the $\sigma^*(C_{sp2}/O\text{-}H)$ orbitals

https://doi.org/10.52111/qnjs.2025.19304

Remarkably, Tables 3a, and 3b also figure out that the change in the electron density of the $\sigma^*(C_{sp2}\text{-H})$ antibonding orbital ($\Delta\sigma^*(C_{sp2}\text{-H})$) become less negative as Z7 goes from O to S to Se and then Te. Therein, the decrease in the electron density at the $\sigma^*(C_{sp2}\text{-H})$ hits bottom when Z7 is O atom, which is explained by the intramolecular hyperconjugative energy (E_{intra}) from n(O7) to $\sigma^*(C_{sp2}\text{-H})$ overcoming the intermolecular hyperconjugative energy of electron density transfer from n(O2) to $\sigma^*(C_{sp2}\text{-H})$, resulting in a rearrangement of electron density throughout **RO2-O7**. Therefore, an increase in occupation of $\sigma^*(C_{sp2}\text{-H})$ orbital causes a lengthening of the C_{sp2}-H bond length and a decrease their stretching frequencies upon complexation. In other words, the stretching frequency of C_{sp2}-H in the nonconventional C_{sp2}-H···Z2 hydrogen bonds tends to turn from blue shift to red shift as Z7 changes from O to Te. For the same Z2 and Z7, the intermolecular transfer of electron density from n(Z2) to $\sigma^*(C_{sp2}\text{-H})$ orbital witnesses an increase according to the substitution of R as the following order: F < H < CH_3. This is consistent with the increase in the proton affinity at Z2 in RCZOH in the order of R: F < H < CH_3 (*cf.* Table 1). This implies that the intermolecular electron density transfer from n(Z2) to $\sigma^*(C_{sp2}\text{-H})$ orbital can be promoted when R varies from an electron-withdrawing group (F) to an electron-donating one (CH_3). When Z2 and Z7 are fixed, the lessening in occupation at $\sigma^*(C_{sp2}\text{-H})$ becomes more pronounced as R changes from H to CH_3 and then F (*cf.* Tables 3a, and 3b). This trend suggests that the characteristic of the nonconventional C_{sp2}-H···Z2 hydrogen bonds shifts gradually from red shift to blue shift when R transitions from an electron-donating group to an electron-withdrawing one.

Regarding the O-H···Z7 hydrogen bonds, there is an increase in the intermolecular electron density transfer from n(Z7) to σ^*(O-H) orbitals when Z2 is replaced by O, S, Se, and Te, respectively. In contrast, for the same R and Z2, the E_{inter} values of O-H···Z7 hydrogen bonds decrease in the sequence of Z7 substituents: O > S > Se > Te. These results agree with the strength tendency of O-H···Z7 as found in AIM analysis. Thus, the intermolecular electron density transfer also affects the strength of O-H···Z7.

It is noted that that the increase in the electron density at σ^*(O-H) in complexes compared to the corresponding monomers ($\Delta\sigma^*$(O-H)) (*ca.* 0.0388-0.0969 e) lengthens the O-H bond length and decreases its stretching frequency, which can induce the red shift of O-H···Z7 hydrogen bonds. For the same Z2 and Z7, the changing of R from CH_3 via H via F results in an improvement in the electron density transfer from n(Z7) to the σ^*(O-H) orbitals, and an increase in the $\Delta\sigma^*$(O-H) values (*cf.* Tables 3a, and 3b). Therefore, the larger strength and red shift of O-H···Z7 hydrogen bonds are gained for R being the electron-withdrawing group (F).

3.4. Changes in bond length and stretching frequency of the O-H and C_{sp2}-H

The change in the bond length (Δr) and stretching frequency ($\Delta\nu$) of the O-H and C_{sp2}-H bonds in the **RZ2-Z7** complexes compared to the corresponding monomers are collected in Tables S3a, and S3b and Figures 2a, and 2b.

The results show the elongation of the O-H bond length and the decrease of its stretching frequency in O-H···Z7 hydrogen bonds following the complexation. Indeed, Δr(O-H) and $\Delta\nu$(O-H) values range from 0.0180 to 0.0482 Å, and from -385.0 to -958.0 cm^{-1}, respectively. This validates the red shift of O-H···Z7 hydrogen bonds as predicted in the NBO analysis above. For the same R and Z2, $\Delta\nu$(O-H) values in the **RZ2-O7** are more negative than those in the **RZ2-S7**, **RZ2-Se7**, and **RZ2-Te7** (*cf.* Figure 2a), implying a larger red shift of O-H···O7 hydrogen bonds compared to O-H···S/Se/Te ones. This is in line with the larger intermolecular electron density transfer from n(O7) to σ^*(O-H) than from n(S7/Se7/Te7) to σ^*(O-H) orbitals (*cf.* Tables 3a, and 3b).

https://doi.org/10.52111/qnjs.2025.19304

This observation, however, differs from the result collected in the complexes of RCZOH with FCHZ. Therein, the O-H red shift of O-H···O hydrogen bonds in the FCHO···RCOOH was less than that of O-H···S hydrogen bonds in the FCHS···RCSOH.[18] Besides, the O-H red shift increases significantly as the F atom in FCHZ monomer is substituted by the NH_2 group. This is due to a strong electron-donating group such as NH_2 surging the electron density at the Z sites in NH_2CHZ. As a result, the Z sites in NH_2CHZ exhibit a higher proton affinity compared to those in FCHZ, and the intermolecular electron density transfers from n(Z) to σ*(O-H) orbital in the RCZOH···NH_2CHZ are larger than those in the RCZOH···FCHZ. Notably, the red shift of O-H···Z hydrogen bonds in the RCZOH···NH_2CHZ complexes is even more significant than that in the RCZOH···CH_3CHZ.[15] This substantially large shift affirms the outstanding influence of a strong electron-donating substituent (NH_2) in NH_2CHZ on the O-H red shift. Figure 2a points out that for the same R and Z7, the O-H red shift in investigated complexes increases in the order of Z2: O < S < Se < Te. This agrees well with the rise in the occupation at the σ*(O-H) orbitals (*cf.* Tables 3a, and 3b) and the polarity of O-H bond in RCZOH (*cf.* Table 1) when Z2 shifts from O to S to Se and then Te. In the case of fixing Z2 and Z7, the red shift of O-H···Z7 hydrogen bonds witness a decline in the sequence **FZ2-Z7** > **HZ2-Z7** > **CH_3Z2-Z7** (*cf.* Figure 2a), being consistent with the decrease in the E_{inter} values of O-H···Z7 hydrogen bonds when R changes from F to CH_3 (*cf.* Tables 3a, and 3b). This trend emphasizes the more dominant role of the electron-withdrawing group (F) relative to the electron-donating one (CH_3) in promoting the O-H red shift. Such observation was once determined in the interaction between XCHZ and YCOOH, where X= H, CH_3, NH_2, and Y= H, F, Cl, Br, CH_3, NH_2 calculated at the same level of theory.[24] The polarity of the O-H bonds in FCZOH is also better than that in HCZOH and CH_3CZOH (*cf.* Table 1). Accordingly, the red shift of O-H···Z7 hydrogen bonds is closely related to the increase in the polarity of the O-H bond in the RCZOH monomers, and the strong intermolecular electron density transfer from n(Z7) to σ*(O-H) orbitals upon complexation.

(a)

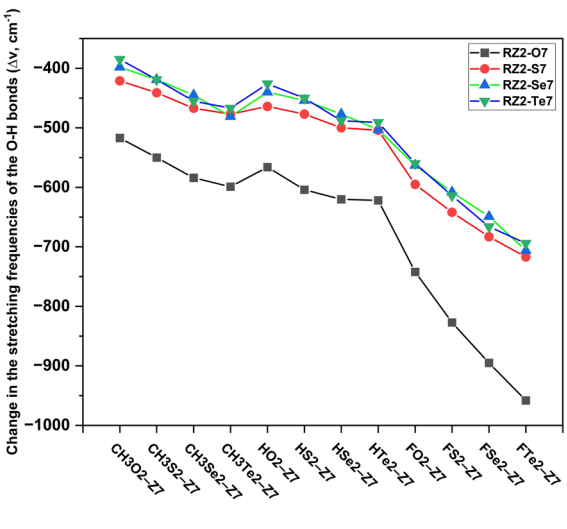

(b)

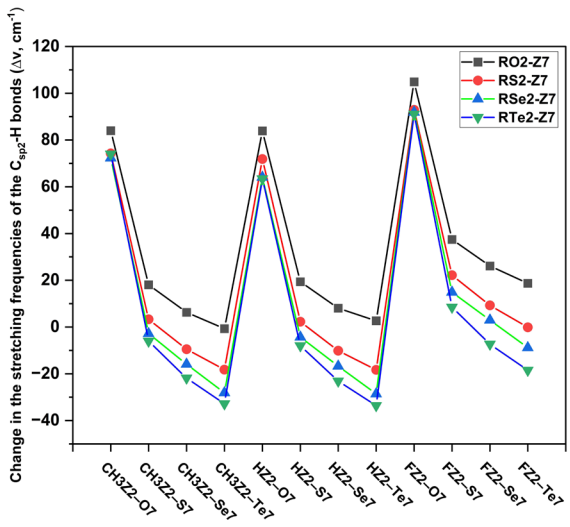

Figure 2. (a) Change in the stretching frequency of the O-H bond in the **RZ2-Z7** complexes compared to the RCZOH monomers, with R= H, F, CH_3; Z (Z2, Z7) = O, S, Se, Te. (b) Change in the stretching frequency of the C_{sp2}-H in the **RZ2-Z7** complexes compared to the NH_2CHZ monomers, with R= H, F, CH_3; Z (Z2, Z7)= O, S, Se, Te.

https://doi.org/10.52111/qnjs.2025.19304

On the other hand, Figure 2b shows that for the same R and Z7, the stretching frequency of C_{sp2}-H involving nonconventional C_{sp2}-H···O2 hydrogen bonds increases during the formation of **RO2-Z7** complexes ($\Delta\nu(C_{sp2}\text{-H}) = 2.7 – 104.9$ cm^{-1}), indicating the C_{sp2}-H blue shift in C_{sp2}-H···O2 hydrogen bonds. This blue shift can be attributed to a reduction of the electron density at the $\sigma^*(C_{sp2}\text{-H})$ orbital following the **RO2-Z7** complexation (*cf.* Tables 3a, and 3b) that leads to a contraction in the bond length and an increase in the stretching frequency of the C_{sp2}-H bond in the C_{sp2}-H···O2. When Z2 is replaced with S, Se, and Te, the C_{sp2}-H stretching frequencies in C_{sp2}-H···S2/Se2/Te2 hydrogen bonds in most complexes tend to be red-shifted, except for **RS2-O7**, **RS2-S7**, **RSe2-O7**, **RSe2-S7**, **RTe2-O7**, and **RTe2-S7**. Therefore, the C_{sp2}-H stretching frequencies of C_{sp2}-H···Z2 hydrogen bonds turn from blue- to red shift as Z2 varies from O to S to Se and then Te. This tendency is proportional to the enhancement of the proton affinity at Z2 in the order O < S < Se < Te (*cf.* Table 1). For the same R and Z2, there is a growth in the C_{sp2}-H red shift upon the substitution of Z7 from O to Te which accords with the rise in the C_{sp2}-H polarity of the NH_2CHZ monomers in the order $NH_2CHO < NH_2CHS < NH_2CHSe < NH_2CHTe$ (*cf.* Table 1). Therefore, the C_{sp2}-H red shift in C_{sp2}-H···Z2 is closely related to the increase in the proton affinity at the Z sites and the polarity of the C_{sp2}-H donor fragment. This observation was also suggested in some previous reports.[15,16,19,24] When fixing Z2 and Z7, the magnitude of the C_{sp2}-H blue shift in C_{sp2}-H···O2 significantly increases in the order of the R substituents: CH_3 < H < F, corresponding to the decrease in the proton affinity at Z site according to the trend above. Hence, the blue shift of C_{sp2}-H bond can be observed along with the decline in the proton affinity at the proton acceptor Z. In comparison with the complexes of the RCZOH with the CH_3/FCHZ, the blue shift of C_{sp2}-H···O is presented more obvious when an electron-donating atom (F) or a weaker electron-donating group (CH_3) in the chalcogenoaldehyde derivatives is replaced with a strong electron-donating substituent (NH_2).[15, 18] This trend relates to the decrease in the polarity of the C_{sp2}-H bonds in the order of chalcogenoaldehyde derivatives: FCHZ > CH_3CHZ > NH_2CHZ. Besides, the C_{sp2}-H stretching-frequencies in C_{sp2}-H···S2/Se2/Te2 hydrogen bonds turn from red shift to blue shift when R changes from H to CH_3 and then F. This observation suggests that the electron-donating group can urge forward the red shift of C_{sp2}-H···Z hydrogen bonds more than the electron-withdrawing one.

4. CONCLUSIONS

There are 48 stable complexes formed between RCZOH and NH_2CHZ (**RZ2-Z7**) (with R= H, F, CH_3; Z= O, S, Se, Te) whose structures are stabilized by O-H···Z7 and C_{sp2}-H···Z2 hydrogen bonds, in which the formers play a predominant role in the stability of the complexes. The increase in the stability of **RZ2-Z7** is observed when R changes from the electron-donating CH_3 group to the electron-withdrawing F one, and Z2 turnes from O to Te. For Z7 being O, S, and Se, **RTe2-Z7** is higher in stability than **RS2-Z7**, **RSe2-Z7**, and **RO2-Z7** while the **RO2-Te7** is more stable than the **RSe2-Te7**, **RS2-Te7**, and **RTe2-Te7**.

The strength of O-H···Z7 hydrogen bonds (*ca.* -16.0 ÷ -101.3 $kJ.mol^{-1}$) is larger than those of C_{sp2}-H···Z2 ones (*ca.* -5.3 ÷ -16,4 $kJ.mol^{-1}$). The O-H stretching frequencies in the O-H···Z7 are characterised by the red shift. The strength and the red shift of O-H···Z7 decrease in the order of Z7 substituents: O > S > Se > Te. In contrast, the change of Z2 from O to Te, and R from CH_3 to F leads to an increase in the O-H red shift. Remarkably, the O-H red shift agrees well with the rise in the O-H polarity, and the proton affinity at the proton acceptors Z. The very strong intermolecular transfer of electron density from n(Z7) to σ^*(O-H) orbitals also contributes significantly to the strength and the red shift of O-H···Z7 hydrogen bonds.

The nonconventional C_{sp2}-H···Z2 hydrogen bonds experience a decrease in their stability as Z2 in RCZOH goes from O to Te, and R changes

https://doi.org/10.52111/qnjs.2025.19304

from CH_3 to F. The substitution of the O atom in NH_2CHZ with S, Se, and Te results in the larger strength of C_{sp2}-H···Z2 hydrogen bonds. In addition, the stretching frequencies of the C_{sp2}-H bond turn from blue shift to red shift as Z2 and Z7 vary from O to Te, in which the C_{sp2}-H blue shift of C_{sp2}-H···O2 reaching 104.9 cm^{-1}. The magnitude of the C_{sp2}-H red shift becomes more obvious when R goes from F to CH_3 substitution. The increase in the C_{sp2}-H stretching frequencies occurs along with the decrease in both the proton affinity at Z2 sites and the polarity of C_{sp2}-H bonds, and *vice versa*. Interestingly, this work highlights the remarkable impact of NH_2 relative to CH_3/F substitute in chalcogenoaldehydes on the increase in the stretching frequency O-H red- and C_{sp2}-H blue shift involving hydrogen bond.

Acknowledgements

This research is funded by Vietnam Ministry of Education and Training (MOET) under grant number B2024-DQN-01.

REFERENCES

1. J. K. M. Sanders. Book review: chemistry beyond the molecule: supramolecular chemistry. Concepts and perspectives. By J.-M. Lehn, *Angewandte Chemie International Edition in English*, **1995**, *34*(22), 2563.
2. G. A. Jeffrey, W. Saenger. *Hydrogen bonding in biological structures*, Springer Berlin Heidelberg, Berlin, 1991.
3. J. N. H. Reek, B. D. Bruin, S. Pullen, T. J. Mooibroek, A. M. Kluwer, X. Caumes. Transition metal catalysis controlled by hydrogen bonding in the second coordination sphere, *Chemical Reviews,* **2022**, *122*(14), 12308-12369.
4. S. J. Grabowski. *Hydrogen bonding: new insights*, *Vol 3*, Springer, USA, 2006.
5. L. Sobczyk, S. J. Grabowski, T. M. Krygowski. Interrelation between H-Bond and Pi-Electron delocalization, *Chemical Reviews,* **2005**, *105*(10), 3513-3560.
6. X. Chang, Y. Zhang, X. Weng, P. Su, W. Wu, Y. Mo. Red-shifting versus blue shift hydrogen bonds: perspective from ab initio valence bond theory, *The Journal of Physical Chemistry A*, **2016**, *120*(17), 2749-2756.
7. P. Hobza, Z. Havlas. Blue shift hydrogen bonds, *Chemical Reviews*, **2000**, *100*(11), 4253-4264.
8. B. J. V. D. Veken, W. A. Herrebout, R. Szostak, D. N. Shchepkin, Z. Havlas, P. Hobza. The Nature of improper, blue shift hydrogen bonding verified experimentally, *Journal of the American Chemical Society*, **2001**, *123*(49), 12290-12293.
9. L. Pejov, K. Hermansson. On the nature of blueshifting hydrogen bonds: Ab initio and density functional studies of several fluoroform complexes, *The Journal of Chemical Physics*, **2003**, *119*(1), 313-324.
10. Y. Mo, C. Wang, L. Guan, B. Braïda, P. C. Hiberty, W. Wu. On the nature of blueshifting hydrogen bonds, *Chemistry - A European Journal*, **2014**, *20*(27), 8444-8452.
11. N. T. Trung, P. N. Khanh, A. J. P. Carvalho, M. T. Nguyen. Remarkable shifts of C_{sp2}-H and O-H stretching frequencies and stability of complexes of formic acid with formaldehydes and thioformaldehydes, *Journal of Computational Chemistry*, **2019**, *40*(13), 1387-1400.
12. S. Bedoura, H. W. Xi, K. H. Lim. Hydrogen bond nature in formamide ($CYHNH_2\cdots XH$; Y= O, S, Se, Te; X= F, HO, NH_2) complexes at their ground and low-lying excited states, *Journal of Physical Organic Chemistry*, **2014**, *27*(3), 226-236.
13. A. K. Chandra, T. Z. Huyskens. Theoretical investigation of the cooperativity in $CH_3CHO\cdots 2H_2O$, $CH_2FCHO\cdots 2H_2O$, and $CH_3CFO\cdots 2H_2O$ systems, *Journal of Atomic and Molecular Physics,* **2012**, *2012*(1), 754879.
14. A. Karpfen, E. S. Kryachko. Blue-shifted A−H stretching modes and cooperative hydrogen bonding. 1. complexes of substituted formaldehyde with cyclic hydrogen fluoride and water clusters, *The Journal of Physical Chemistry A*, **2007**, *111*(33), 8177-8187.
15. N. T. An, N. T. Duong, N. N. Tri, N. T. Trung. Role of O–H···O/S conventional hydrogen bonds in considerable C_{sp2}–H blue-shift in the binary systems of acetaldehyde and thioacetaldehyde with substituted carboxylic and thiocarboxylic acids, *RSC Advances,* **2022**, *12*(54), 35309-35319.
16. N. T. T. Cuc, N. T. An, V. T. Ngan, A. K. Chandra, N. T. Trung. Importance of water and intramolecular interaction governs substantial blue shift of C_{sp2}–H stretching frequency in

complexes between chalcogenoaldehydes and water, *RSC Advances,* **2022**, *12*(4), 1998-2008.

17. N. T. T. Cuc, C. T. D. Phan, N. T. A. Nhung, M. T. Nguyen, N. T. Trung, V. T. Ngan. Theoretical aspects of nonconventional hydrogen bonds in the complexes of aldehydes and hydrogen chalcogenides, *The Journal of Physical Chemistry A,* **2021**, *125*(48), 10291-10302.
18. L. T. T. Quyen, N. T. Trung. Noticeable characteristics of conventional and nonconventional hydrogen bonds in the binary systems of chalcogenoaldehyde and chalcogenocarboxylic acid derivatives, *RSC Advances*, **2024**, *14*(54), 40018-40030.
19. L. T. T. Quyen, B. N. Tung, P. N. Thach, N. N. Tri, N. T. Trung. Characteristics of nonconventional hydrogen bonds and stability of dimers of chalcogenoaldehyde derivatives: a noticeable role of oxygen compared to other chalcogens, *RSC Advances*, **2024**, *14*(20), 14114-14125.
20. K. K. Mishra, S. K. Singh, P. Ghosh, D. Ghosh, A. Das. The nature of selenium hydrogen bonding: gas phase spectroscopy and quantum chemistry calculations, *Physical Chemistry Chemical Physics*, **2017**, *19*(35), 24179-24187.
21. H. Q. Dai, N. N. Tri, N. T. T. Trang, N. T. Trung. Remarkable effects of substitution on stability of complexes and origin of the C–H···O(N) hydrogen bonds formed between acetone's derivative and CO_2, XCN (X = F, Cl, Br), *RSC Advances*, **2014**, *4*(27), 13901-13908.
22. N. T. H. Man, P. L. Nhan, V. Vo, D. T. Quang, N. T. Trung. An insight into C-H···N hydrogen bond and stability of the complexes formed by trihalomethanes with ammonia and its monohalogenated derivatives, *International Journal of Quantum Chemistry*, **2017**, *117*(6), e25338.
23. N. N. Tri, N. T. H. Man, N. L. Tuan, N. T. T. Trang, D. T. Quang, N. T. Trung. Structure, stability and interactions in the complexes of carbonyls with cyanides, *Theoretical Chemistry Accounts*, **2016**, *136*(1), 10.
24. N. T. An, V. T. Ngan, N. T. Trung. Profound importance of the conventional O–H···O hydrogen bond versus a considerable blue shift of the C_{sp2}–H bond in complexes of substituted carbonyls and carboxyls, *Physical Chemistry Chemical Physics*, **2024**, *26*(34), 22775-22789.
25. M. H. Gordon, J. A. Pople, M. J. Frisch. MP2 energy evaluation by direct methods, *Chemical Physics Letters*, **1988**, *153*(6), 503-506.
26. K. A. Peterson, D. Figgen, E. Goll, H. Stoll, M. Dolg. Systematically convergent basis sets with relativistic pseudopotentials. II. Small-core pseudopotentials and correlation consistent basis sets for the post-d group 16–18 elements, *The Journal of Chemical Physics*, **2003**, *119*(21), 11113-11123.
27. M. J. Frisch. *Gaussian 16/Gaussian*, Published online, 2016.
28. R. F. W. Bader. A quantum theory of molecular structure and its applications, *Chemical Reviews*, **1991**, *91*(5), 893-928.
29. R. F. W. Bader. Atoms in molecules, *Accounts of Chemical Research*, **1985**, *18*(1), 9-15.
30. E. Espinosa, E. Molins, C. Lecomte. Hydrogen bond strengths revealed by topological analyses of experimentally observed electron densities, *Chemical Physics Letters*, **1998**, *285*(3), 170-173.
31. E. D. Glendening, C. R. Landis, F. Weinhold. Natural bond orbital methods, *WIREs Computational Molecular Science*, **2012**, *2*(1), 1-42.
32. U. Koch, P. L. A. Popelier. Characterization of C-H···O hydrogen bonds on the basis of the charge density, *The Journal of Physical Chemistry*, **1995**, *99*(24), 9747-9754.
33. S. Bhattacharyya, A. Bhattacherjee, P. R. Shirhatti, S. Wategaonkar. O–H···S Hydrogen Bonds Conform to the Acid–Base Formalism, *The Journal of Physical Chemistry A*, **2013**, *117*(34), 8238-8250.
34. B. Das, A. Chakraborty, S. Chakraborty. Effect of ionic charge on O-H···Se hydrogen bond: a computational study, *Computational and Theoretical Chemistry,* **2017**, *1102*, 127-138.

https://doi.org/10.52111/qnjs.2025.19304

QUY NHON UNIVERSITY
JOURNAL OF SCIENCE

Supporting information

An insight into stability and characteristics of O/C_{sp2}-H···Z hydrogen bonds in the binary systems of chalcogenocarboxylic acid and formamide derivatives

Le Thi Tu Quyen,[1] Bui Duc Ai,[1] Tran Manh Trung,[1]
Pham Ngoc Thach,[1,2] Nguyen Tien Trung[1,2,*]

[1]Laborabory of Computational Chemistry and Modelling, Quy Nhon University, Vietnam
[2]Faculty of Natural Sciences, Quy Nhon University, Vietnam

**Corresponding author. Email: nguyentientrung@qnu.edu.vn*

Table 1a. The H6···Z2 interaction distance ($r_{H6\cdots Z2}$), selected parameters at BCPs of H6···Z2 interactions, and individual energies (E_{HB}) of the nonconventional C_{sp2}-H···Z2 hydrogen bonds in NH_2CHZ···RCZOH complexes (with R= H, F, CH_3; Z= O, S, Se, Te).

Complex	$r_{H6\cdots Z2}$ (Å)	ρ(r) (au)	$\nabla^2(\rho)$ (au)	H(r) (au)	E_{HB} (kJ.mol^{-1})
CH_3O2–O7	2.29	0.014	0.050	0.0015	-12.4
CH_3S2–O7	2.78	0.011	0.030	0.0009	-7.3
CH_3Se2–O7	2.90	0.010	0.026	0.0008	-6.4
CH_3Te2–O7	3.08	0.009	0.022	0.0006	-5.4
HO2–O7	2.31	0.014	0.048	0.0014	-11.9
HS2–O7	2.79	0.011	0.029	0.0009	-7.1
HSe2–O7	2.91	0.010	0.026	0.0008	-6.2
HTe2–O7	3.08	0.009	0.021	0.0006	-5.3
FO2–O7	2.34	0.013	0.045	0.0014	-11.2
FS2–O7	2.80	0.010	0.029	0.0010	-7.0
FSe2–O7	2.90	0.011	0.026	0.0009	-6.3
FTe2–O7	3.06	0.010	0.022	0.0007	-5.6
CH_3O2–S7	2.17	0.017	0.061	0.0016	-15.8
CH_3S2–S7	2.65	0.013	0.034	0.0008	-9.3
CH_3Se2–S7	2.77	0.012	0.030	0.0007	-8.1
CH_3Te2–S7	2.95	0.012	0.025	0.0005	-6.7
HO2–S7	2.19	0.016	0.059	0.0016	-15.2
HS2–S7	2.66	0.013	0.034	0.0008	-9.1
HSe2–S7	2.78	0.012	0.030	0.0007	-8.1
HTe2–S7	2.96	0.011	0.024	0.0005	-6.6
FO2–S7	2.22	0.015	0.056	0.0017	-13.9

Complex	$r_{H6\cdots Z2}$ (Å)	ρ(r) (au)	$\nabla^2(\rho)$ (au)	H(r) (au)	E_{HB} (kJ.mol^{-1})
FS2–S7	2.68	0.012	0.033	0.0009	-8.6
FSe2–S7	2.79	0.012	0.030	0.0008	-7.6
FTe2–S7	2.95	0.011	0.025	0.0006	-6.6
CH_3O2–Se7	2.15	0.017	0.063	0.0017	-16.3
CH_3S2–Se7	2.65	0.013	0.035	0.0007	-9.5
CH_3Se2–Se7	2.76	0.013	0.030	0.0007	-8.2
CH_3Te2–Se7	2.94	0.012	0.025	0.0005	-6.9
HO2–Se7	2.17	0.017	0.060	0.0016	-15.6
HS2–Se7	2.65	0.013	0.034	0.0007	-9.3
HSe2–Se7	2.77	0.012	0.032	0.0006	-8.3
HTe2–Se7	2.94	0.012	0.025	0.0005	-6.9
FO2–Se7	2.20	0.015	0.057	0.0018	-14.2
FS2–Se7	2.68	0.012	0.033	0.0009	-8.7
FSe2–Se7	2.78	0.012	0.030	0.0008	-7.7
FTe2–Se7	2.94	0.012	0.025	0.0006	-6.8
CH_3O2–Te7	2.15	0.017	0.063	0.0017	-16.4
CH_3S2–Te7	2.63	0.013	0.035	0.0007	-9.7
CH_3Se2–Te7	2.72	0.013	0.032	0.0007	-8.9
CH_3Te2–Te7	2.93	0.012	0.025	0.0005	-7.0
HO2–Te7	2.17	0.017	0.061	0.0016	-15.7
HS2–Te7	2.64	0.013	0.034	0.0007	-9.5
HSe2–Te7	2.73	0.013	0.032	0.0007	-8.7
HTe2–Te7	2.94	0.012	0.025	0.0005	-6.9
FO2–Te7	2.20	0.015	0.058	0.0018	-14.1
FS2–Te7	2.67	0.012	0.034	0.0009	-8.8
FSe2–Te7	2.75	0.0123	0.031	0.0008	-8.2
FTe2–Te7	2.94	0.011	0.025	0.0006	-6.7

Table 1b. The H4···Z7 interaction distance ($r_{H6\cdots Z2}$), selected parameters at BCPs of H4···Z7 interactions, and individual energies (E_{HB}) of the O-H···Z7 hydrogen bonds in NH_2CHZ···RCZOH complexes (with R= H, F, CH_3; Z= O, S, Se, Te).

Complex	$r_{H6\cdots Z2}$ (Å)	ρ(r) (au)	$\nabla^2(\rho)$ (au)	H(r) (au)	E_{HB} (kJ.mol^{-1})
CH_3O2–O7	1.689	0.047	0.102	-0.011	-61.8
CH_3S2–O7	1.655	0.050	0.106	-0.013	-68.1
CH_3Se2–O7	1.638	0.052	0.108	-0.014	-71.8
CH_3Te2–O7	1.627	0.053	0.109	-0.015	-74.2
HO2–O7	1.668	0.049	0.103	-0.012	-66.2
HS2–O7	1.640	0.052	0.106	-0.014	-71.7
HSe2–O7	1.626	0.054	0.107	-0.015	-75.0
HTe2–O7	1.622	0.054	0.109	-0.015	-75.7

https://doi.org/10.52111/qnjs.2025.19304

Complex	$r_{H6\cdots Z2}$ (Å)	ρ(r) (au)	$\nabla^2(\rho)$ (au)	H(r) (au)	E_{HB} (kJ.mol^{-1})
FO2–O7	1.605	0.057	0.108	-0.018	-81.4
FS2–O7	1.571	0.062	0.109	-0.021	-89.9
FSe2–O7	1.550	0.065	0.109	-0.023	-95.9
FTe2–O7	1.533	0.068	0.109	-0.025	-101.3
CH_3O2–S7	2.216	0.029	0.046	-0.005	-27.0
CH_3S2–S7	2.192	0.031	0.046	-0.005	-28.8
CH_3Se2–S7	2.176	0.032	0.046	-0.006	-30.1
CH_3Te2–S7	2.169	0.032	0.046	-0.006	-30.8
HO2–S7	2.193	0.031	0.045	-0.005	-28.9
HS2–S7	2.173	0.032	0.045	-0.006	-30.5
HSe2–S7	2.159	0.033	0.045	-0.006	-30.1
HTe2–S7	2.156	0.033	0.045	-0.007	-31.9
FO2–S7	2.129	0.035	0.044	-0.008	-34.5
FS2–S7	2.109	0.037	0.042	-0.009	-36.3
FSe2–S7	2.094	0.038	0.041	-0.009	-37.9
FTe2–S7	2.085	0.039	0.040	-0.010	-38.9
CH_3O2–Se7	2.358	0.025	0.039	-0.003	-21.6
CH_3S2–Se7	2.331	0.027	0.039	-0.004	-23.2
CH_3Se2–Se7	2.315	0.028	0.038	-0.004	-24.3
CH_3Te2–Se7	2.278	0.030	0.039	-0.005	-26.8
HO2–Se7	2.334	0.027	0.039	-0.004	-23.2
HS2–Se7	2.312	0.028	0.038	-0.005	-24.6
HSe2–Se7	2.298	0.030	0.038	-0.005	-26.0
HTe2–Se7	2.267	0.031	0.038	-0.006	-27.7
FO2–Se7	2.269	0.031	0.037	-0.006	-27.8
FS2–Se7	2.249	0.032	0.036	-0.007	-29.3
FSe2–Se7	2.234	0.033	0.035	-0.007	-30.5
FTe2–Se7	2.199	0.036	0.034	-0.008	-33.3
CH_3O2–Te7	2.562	0.022	0.030	-0.002	-16.0
CH_3S2–Te7	2.524	0.024	0.030	-0.003	-17.8
CH_3Se2–Te7	2.501	0.025	0.030	-0.003	-18.9
CH_3Te2–Te7	2.490	0.026	0.030	-0.004	-19.5
HO2–Te7	2.539	0.023	0.030	-0.003	-17.1
HS2–Te7	2.509	0.025	0.030	-0.003	-18.6
HSe2–Te7	2.486	0.026	0.029	-0.004	-19.8
HTe2–Te7	2.480	0.026	0.029	-0.004	-20.1
FO2–Te7	2.463	0.027	0.029	-0.004	-21.1
FS2–Te7	2.435	0.029	0.028	-0.005	-22.8
FSe2–Te7	2.416	0.030	0.026	-0.006	-24.0
CH_3O2–Te7	2.406	0.031	0.026	-0.006	-24.6

Table S2. NBO charge at H4, H6, Z2, and Z7 atoms in **RZ2-Z7** complexes with R= H, F, CH_3; Z2(Z7) = O, S, Se, Te.

	CH_3O-O	CH_3S-O	CH_3Se-O	CH_3Te-O		CH_3O-Se	CH_3S-Se	CH_3Se-Se	CH_3Te-Se
q(H4)	0.540	0.547	0.551	0.554	**q(H4)**	0.517	0.524	0.528	0.528
q(Z7)	-0.770	-0.770	-0.773	-0.776	**q(Z7)**	-0.231	-0.215	-0.214	-0.204
q(H6)	0.149	0.138	0.140	0.140	**q(H6)**	0.213	0.201	0.201	0.202
q(Z2)	-0.762	-0.264	-0.238	-0.166	**q(Z2)**	-0.759	-0.245	-0.215	-0.139
	HO-O	**HS-O**	**HSe-O**	**HTe-O**		**HO-Se**	**HS-Se**	**HSe-Se**	**HTe-Se**
q(H4)	0.541	0.545	0.549	0.553	**q(H4)**	0.515	0.520	0.523	0.522
q(Z7)	-0.772	-0.771	-0.774	-0.777	**q(Z7)**	-0.227	-0.211	-0.170	-0.201
q(H6)	0.147	0.138	0.139	0.138	**q(H6)**	0.211	0.199	0.173	0.200
q(Z2)	-0.748	-0.254	-0.225	-0.147	**q(Z2)**	-0.744	-0.233	-0.128	-0.119
	FO-O	**FS-O**	**FSe-O**	**FTe-O**		**FO-Se**	**FS-Se**	**FSe-Se**	**FTe-Se**
q(H4)	0.552	0.559	0.562	0.566	**q(H4)**	0.524	0.531	0.534	0.532
q(Z7)	-0.775	-0.774	-0.776	-0.780	**q(Z7)**	-0.216	-0.200	-0.199	-0.189
q(H6)	0.147	0.140	0.143	0.145	**q(H6)**	0.208	0.198	0.200	0.202
q(Z2)	-0.751	-0.275	-0.254	-0.195	**q(Z2)**	-0.747	-0.252	-0.226	-0.161
	CH_3O-S	CH_3S-S	CH_3Se-S	CH_3Te-S		CH_3O-Te	CH_3S-Te	CH_3Se-Te	CH_3Te-Te
q(H4)	0.516	0.524	0.527	0.529	**q(H4)**	0.516	0.523	0.526	0.528
q(Z7)	-0.259	-0.246	-0.246	-0.246	**q(Z7)**	-0.160	-0.137	-0.135	-0.133
q(H6)	0.211	0.199	0.200	0.199	**q(H6)**	0.210	0.197	0.198	0.198
q(Z2)	-0.759	-0.246	-0.215	-0.138	**q(Z2)**	-0.760	-0.244	-0.207	-0.135
	HO-S	**HS-S**	**HSe-S**	**HTe-S**		**HO-Te**	**HS-Te**	**HSe-Te**	**HTe-Te**
q(H4)	0.515	0.519	0.522	0.524	**q(H4)**	0.514	0.518	0.520	0.522
q(Z7)	-0.256	-0.243	-0.243	-0.244	**q(Z7)**	-0.154	-0.132	-0.130	-0.129
q(H6)	0.210	0.197	0.198	0.197	**q(H6)**	0.208	0.195	0.196	0.196
q(Z2)	-0.743	-0.234	-0.202	-0.119	**q(Z2)**	-0.744	-0.231	-0.193	-0.115
	FO-S	**FS-S**	**FSe-S**	**FTe-S**		**FO-Te**	**FS-Te**	**FSe-Te**	**FTe-Te**
q(H4)	0.522	0.530	0.532	0.533	**q(H4)**	0.523	0.530	0.531	0.532
q(Z7)	-0.247	-0.234	-0.234	-0.235	**q(Z7)**	-0.138	-0.115	-0.113	-0.112
q(H6)	0.207	0.197	0.199	0.200	**q(H6)**	0.204	0.194	0.196	0.197
q(Z2)	-0.746	-0.253	-0.227	-0.161	**q(Z2)**	-0.747	-0.251	-0.218	-0.157

https://doi.org/10.52111/qnjs.2025.19304

Table S3a. The change in the bond length (Δr, Å) and stretching frequency (Δν, cm^{-1}) of C_{sp2}-H and O-H bonds in the **RZ2-Z7** complexes compared to their corresponding monomers, with R= H, F, CH_3; Z2= O, S, Se, Te; Z7 = O, S.

	CH_3O2-O7	**CH_3S2-O7**	**CH_3Se2-O7**	**CH_3Te2-O7**
Δr(C_{sp2}-H)	-0.0060	-0.0059	-0.0060	-0.0063
Δν(C_{sp2}-H)	84	74.3	72.3	74.0
Δr(O-H)	0.0256	0.0273	0.0291	0.0300
Δν(O-H)	-517	-550	-584	-599
	HO2-O7	**HS2-O7**	**HSe2-O7**	**HTe2-O7**
Δr(C_{sp2}-H)	-0.0059	-0.0059	-0.0058	-0.0060
Δν(C_{sp2}-H)	83.9	71.9	64.1	63.4
Δr(O-H)	0.0283	0.0295	0.0311	0.0311
Δν(O-H)	-566	-604	-620	-622
	FO2-O7	**FS2-O7**	**FSe2-O7**	**FTe2-O7**
Δr(C_{sp2}-H)	-0.0069	-0.0071	-0.0072	-0.0075
Δν(C_{sp2}-H)	104.9	92.9	91.9	91.1
Δr(O-H)	0.0368	0.0411	0.0447	0.0482
Δν(O-H)	-742	-827	-895	-958
	CH_3O2-S7	**CH_3S2-S7**	**CH_3Se2-S7**	**CH_3Te2-S7**
Δr(C_{sp2}-H)	-0.0005	-0.0002	0.0000	-0.0002
Δν(C_{sp2}-H)	18.1	3.3	-2.8	-6.0
Δr(O-H)	0.0202	0.0212	0.0225	0.0231
Δν(O-H)	-421	-441	-467	-477
	HO2-S7	**HS2-S7**	**HSe2-S7**	**HTe2-S7**
Δr(C_{sp2}-H)	-0.0006	-0.0002	0.0001	-0.0001
Δν(C_{sp2}-H)	19.4	2.3	-4.3	-8.0
Δr(O-H)	0.0224	0.0231	0.0244	0.0247
Δν(O-H)	-464	-477	-500	-504
	FO2-S7	**FS2-S7**	**FSe2-S7**	**FTe2-S7**
Δr(C_{sp2}-H)	-0.0019	-0.0016	-0.0013	-0.0013
Δν(C_{sp2}-H)	37.5	22.2	14.9	8.5
Δr(O-H)	0.0288	0.0308	0.0328	0.0346
Δν(O-H)	-595	-642	-683	-717

Table S3b. The change in the bond length (Δr, Å) and stretching frequency (Δν, cm^{-1}) of C_{sp2}-H and O-H bonds in the **RZ2-Z7** complexes compared to their corresponding monomers, with R= H, F, CH_3, Z2= O, S, Se, Te; Z7= Se, Te.

	CH_3O2-Se7	CH_3S2-Se7	CH_3Se2-Se7	CH_3Te2-Se7
Δr(C_{sp2}-H)	0.0004	0.0007	0.0009	0.0009
Δν(C_{sp2}-H)	6.3	-9.5	-15.9	-21.8
Δr(O-H)	0.0190	0.0201	0.0214	0.0233
Δν(O-H)	-398	-419	-445	-481
	HO2-Se7	**HS2-Se7**	**HSe2-Se7**	**HTe2-Se7**
Δr(C_{sp2}-H)	0.0002	0.0007	0.0010	0.0010
Δν(C_{sp2}-H)	8.1	-10.1	-16.7	-23.1
Δr(O-H)	0.0212	0.0219	0.0232	0.0247
Δν(O-H)	-440	-454	-477	-503
	FO2-Se7	**FS2-Se7**	**FSe2-Se7**	**FTe2-Se7**
Δr(C_{sp2}-H)	-0.0011	-0.0006	-0.0003	-0.0001
Δν(C_{sp2}-H)	26.1	9.3	3.0	-7.3
Δr(O-H)	0.0272	0.0290	0.0310	0.0341
Δν(O-H)	-563	-608	-649	-706
	CH_3O2-Te7	CH_3S2-Te7	CH_3Se2-Te7	CH_3Te2-Te7
Δr(C_{sp2}-H)	0.0009	0.0013	0.0018	0.0017
Δν(C_{sp2}-H)	-0.7	-18.2	-28.1	-32.8
Δr(O-H)	0.0180	0.0196	0.0214	0.0220
Δν(O-H)	-385	-419	-455	-467
	HO2-Te7	**HS2-Te7**	**HSe2-Te7**	**HTe2-Te7**
Δr(C_{sp2}-H)	0.0006	0.0013	0.0018	0.0018
Δν(C_{sp2}-H)	2.7	-18.3	-28.6	-33.6
Δr(O-H)	0.0200	0.0212	0.0232	0.0234
Δν(O-H)	-426	-450	-488	-491
	FO2-Te7	**FS2-Te7**	**FSe2-Te7**	**FTe2-Te7**
Δr(C_{sp2}-H)	-0.0005	0.0001	0.0006	0.0008
Δν(C_{sp2}-H)	18.7	-0.1	-8.8	-18.5
Δr(O-H)	0.0264	0.0288	0.0312	0.0327
Δν(O-H)	-560	-614	-666	-694

https://doi.org/10.52111/qnjs.2025.19304

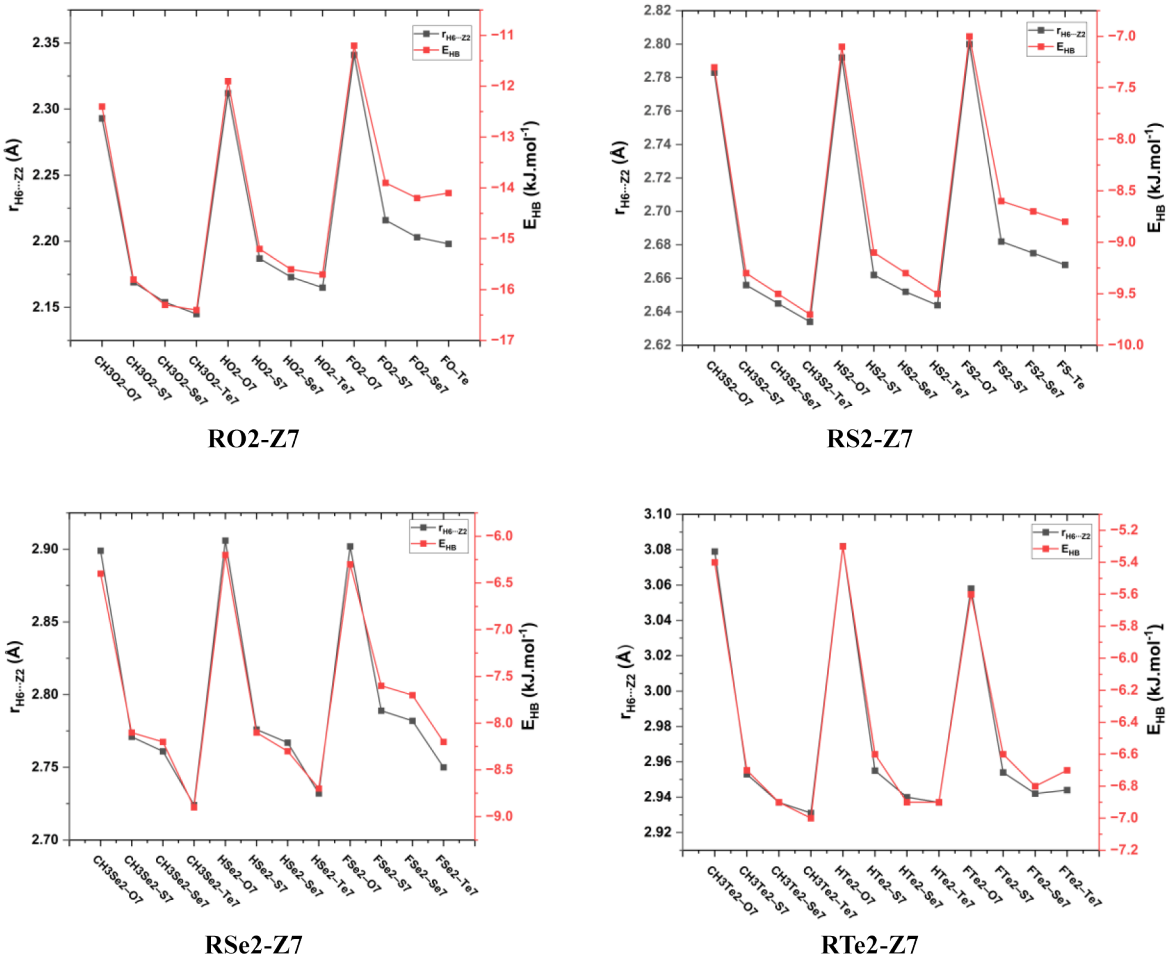

Figure S1a. The relationship between the H6···Z2 interaction distance and individual energy (E_{HB}) of C_{sp2}-H···Z2 hydrogen bond in **RZ2-Z7** complexes (with R= H, F, CH_3; Z2(Z7) = O, S, Se, Te).

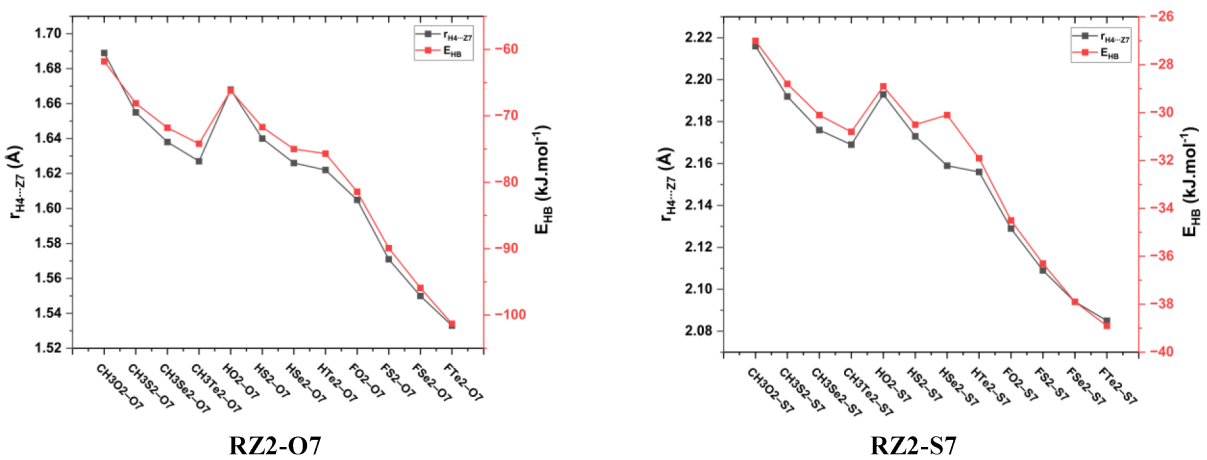

https://doi.org/10.52111/qnjs.2025.19304

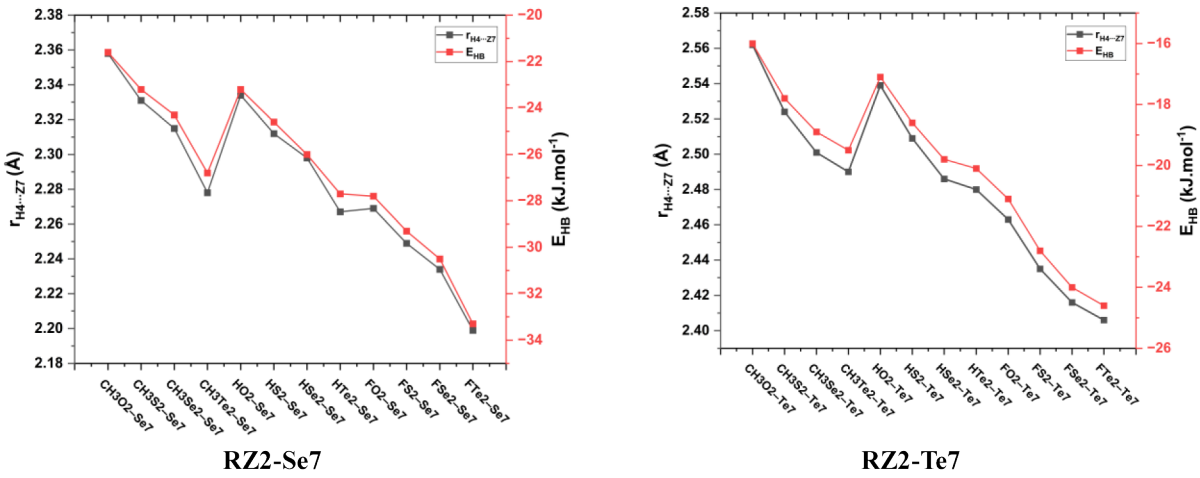

Figure S1b. The relationship between the H4···Z7 interaction distance and individual energy (E_{HB}) of O-H···Z7 hydrogen bond in **RZ2-Z7** complexes (with R= H, F, CH_3; Z2(Z7) = O, S, Se, Te).

https://doi.org/10.52111/qnjs.2025.19304